Optimization and Determination of Process Parameters in Thin Film SOI Photo-BJMOSFET

Hai-Qing Xie, Yun Zeng*, Yong-Hong Yan, Guo-Liang Zhang, Tai-Hong Wang

Abstract—We propose photo-BJMOSFET (Bipolar Junction Metal-Oxide-Semiconductor Field Effect Transistor) fabricated on SOI film. ITO film is adopted in the device as gate electrode to reduce light absorption. I-V characteristics of photo-BJMOSFET obtained in dark (dark current) and under 570nm illumination (photo current) are studied furthermore to achieve high photo-to-dark-current contrast ratio. Two variables in the calculation were the channel length and the thickness of the film which were set equal to six different values, i.e., L=2, 4, 6, 8, 10, and 12μm and three different values, i.e., d_{si}=100, 200 and 300nm, respectively. The results indicate that the greatest photo-to-dark-current contrast ratio is achieved with L=10μm and d_{si}=200 nm at V_{GK}=0.6V.

Keywords—Photo-to-dark-current contrast ratio, Photo-current, Dark-current, Process parameter

I. INTRODUCTION

NOWADAYS, short distance optical communications and emerging optical storage(OS) systems such as DVD applications require fast (gigahertz to tens of gigahertz bandwidth) and responsive photodetectors with high photo-to-dark-current ratio increasingly[1]-[4]. Bulk silicon detectors, however, hardly cope with these specifications, mainly in regards to bandwidth, and nonintegrated detectors are usually used due to high dark currents of photodiode and low sensitivity of MOS structure(due to only one kind of carrier and light-absorption of gate) in CMOS process under 0.25μm[5]-[9]. This limits the ultimate performances of optical receivers circuits because of high bonding capacitor, cost, and area, which is a limitation for the deployment of local-area networks, interchip/intrachip interconnects, and for the first mile ethernet[10].

In order to achieve low dark current and high photo-current under low reverse voltage, photo-BJMOSFET (Bipolar Junction Metal-Oxide-Semiconductor Field Effect Transistor) based on SOI film compatible with CMOS process was proposed. The structure of photo-BJMOSFET is very similar to traditional MOS structure, but only ITO is applied as gate to reduce light absorption. Recombination was reduced due to depletion but not inversion region of thin film under gate

Hai-Qing Xie is with the School of Physics and Microelectronics Science, Hunan University, Changsha 410082, P.R.China (e-mail: xiehaiqing@gmail.com).
Yun Zeng is with the School of Physics and Microelectronics Science, Hunan University, Changsha 410082, P.R.China (Tel.: +86 731 8822332; fax: +86 731 8822332 e-mail: zengyun@hnu.cn)

voltage (but not high reverse voltage) to obtain low dark current and high photo-current. Consequently, it can get high sensitivity and responsibility.

In this paper, I-V characteristics of photo-BJMOSFET obtained in dark (dark current) and under 570nm illumination (photo current) are studied furthermore. Two variables in the calculation were the channel length and the thickness of the film which were set equal to six different values, i.e., L=2, 4, 6, 8, 10, and 12μm and three different values, i.e., d_{si}=100, 200 and 300nm, respectively.

II. DEVICE STRUCTURE

Thin film SOI photo-BJMOSFET realized in 0.18μm SOI CMOS technology with the parameters shown in Fig.1. It is seen that the structure is very similar to that of traditional NMOS except a P^+N injection junction is formed by using P^+ region instead of N^+ region as drain. Furthermore, ITO is adopted as gate electrode to reduce the absorption loss of traditional gate. The thin Si film thickness, d_{si}, is equal to three different values, i.e., d_{si}=100, 200 and 300nm, the front oxide thickness, d_{FOX}, is equal to 80nm , the buried oxide (BOX) thickness, d_{BOX}, is equal to 380nm and the thickness of substrate, d_{sub}, is equal to 500nm. The length of the N^+ and P^+ zones, L_{PN}, is equal to 1μm and L, the length of the channel which typically corresponds to a P$^-$-doping of 10^{15}cm^{-3}, is equal to six different values, i.e., L=2, 4, 6, 8, 10 and 12μm.
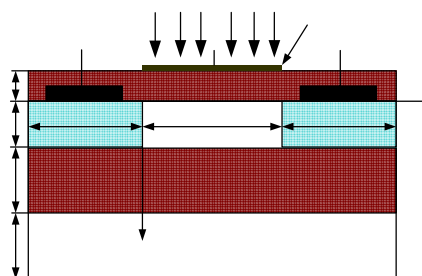

Fig. 1 Schematic cross-section of thin film SOI photo-BJMOSFET.

The absorption in ITO film is the main loss of incident light. The deposition of ITO was performed in a vacuum chamber, where the preliminary pressure was 1×10^{-3}Pa. Sputtering was done at a pressure of 0.5Pa, at a constant power of 100W. During the sputtering process, the temperature of the substrates always was kept at 150 for 1.5 hours. The measurement of

Yong-Hong Yan is with the School of Physics and Microelectronics Science, Hunan University, Changsha 410082, P.R.China (e-mail: yyh@hnu.cn).

World Academy of Science, Engineering and Technology
International Journal of Physical and Mathematical Sciences
Vol:3, No:10, 2009

transmittancea to the wavelength of ITO film is presented in Fig.2. It can be seen that the transmittance of ITO film is higher than 80% for λ from 500nm to 700nm, and can be adopted as gate electrode to reduce light absorption.
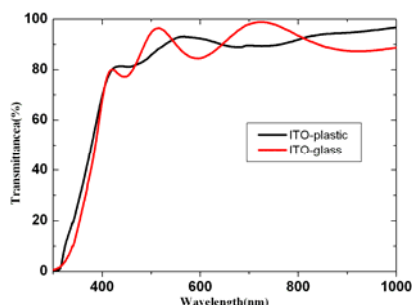

Fig. 2 Transmittancea to wavelength of ITO film which was deposited on glass and plastic, respectively, with thickness is 100nm.

In photo-BJMOSFET, the depletion but not inversion region is formed by V_{GK} (the voltage between electrode G and electrode K) under lower V_{AK} (the voltage between electrode A and electrode K) in channel to decrease dark current and increase internal quantum efficiency.

In photo-BJMOSFET, we can obtain the Boltzmann distribution

$$n_{surface} = n_i e^{(\psi_s(x) - \phi_F)/\phi_T} \tag{1}$$

where $n_{surface}$, n_i, $\psi_s(x)$, respectively, are the electron concentration at the surface, the intrinsic concentration, surface potential at x position.

The quantity of charge per unit area in the semiconductor under oxide Q_C is given by

$$Q_C = -\sqrt{2q\varepsilon_s N_A}$$
$$\times \sqrt{V_t e^{-\psi_S/\phi_T} + \psi_S - \phi_T + e^{-2\phi_f/\phi_T}(\phi_T e^{\psi_S/\phi_T} - \psi_S - \phi_T)} \tag{2}$$

where q, ε_s, N_A, ψ_S, ϕ_f and ϕ_T, are the magnitude of the electron charge, permittivity of the material, doping concentration, surface potential, Fermi potential of the material, and thermal voltage, respectively.

Expression for V_{GK} can be obtained using Kirchhoff's voltage law

$$V_{GK} = V_{FB} + \psi_S$$
$$+ \gamma\sqrt{\phi_T e^{-\psi_S/\phi_T} + \psi_S - \phi_T + e^{-2\phi_f/\phi_T}(\phi_T e^{\psi_S/\phi_T} - \psi_S - \phi_T)} \tag{3}$$

where V_{FB} is the flat-band voltage, the expression for γ is as follows:

$$\gamma = \frac{\sqrt{2q\varepsilon_s N_A}}{C_{OX}} \tag{4}$$

where C_{OX} is the oxide capacitance per unit area.

In depletion region (which photo-BJMOSFET operating in), $n_{surface}$ is not larger than n_i. The charge due to the electrons in

the inversion layer Q_L can be ignored based on ideal assumption.

Thus, Equation (3) can be simplified as follows:

$$V_{GK} \approx V_{FB} + \psi_S + \gamma\sqrt{\psi_S} \tag{5}$$

then

$$\psi_S = \left(-\frac{\gamma}{2} + \sqrt{\frac{\gamma^2}{4} + V_{GK} - V_{FB}}\right)^2 \tag{6}$$

III. DEVICE SIMULATION AND DISCUSSION

Numerical simulation studies were conducted by using a two-dimensional (2D) device analysis program (ATLAS by SILVACO, Inc.) implemented on a WINDOWS system [11]. This software solves the coupled semiconductor equations, Poisson's equation, and the electron and hole continuity equations. Through simulation, the field equations of the problem were solved numerically without simplifying approximations regarding the distribution and pattern of the physical mechanisms involved. (In this regard, simulation results are considered more to be dependable than the exact closed form solutions obtained from oversimplified idealizations of the actual problem.)

To obtain improved resolution in the regions of interest, the simulation required a very fine mesh in thin film where steep gradients in the electrical field were anticipated. A total of 19332 grid nodes and 38092 elements (triangles) were used in modeling the intermediate length sample (L=10μm) with a commensurate increase/decrease in the number of nodes and elements for the longer and shorter samples, respectively. Gummel-Newton-based numerical algorithms were implemented and used by the simulation program in order to solve the discretized form of the field equations [12].

In order to understand the behavior of the current in the depletion region, it was essential to study in detail the volume distribution of the carriers for the entire thin film. Simulation results for the electron and hole concentrations are given in Fig.3. The data were taken from the cut line taken from the front interface to the back interface by utilizing a cut line at the middle of the channel, where zero in Fig.3 is taken to be at the front interface. For different channel length, the concentration of electrons at front interface is lower than 10^{15}cm^{-3} at V_{GK}=1V. In other words, whole thin film is in depletion region at V_{GK}=1V, which is consistent with (6). It is also indicated in Fig.3 that the concentration of electrons at front interface in L=2μm is lower than that in other channel length due to the influence of V_{AK}.
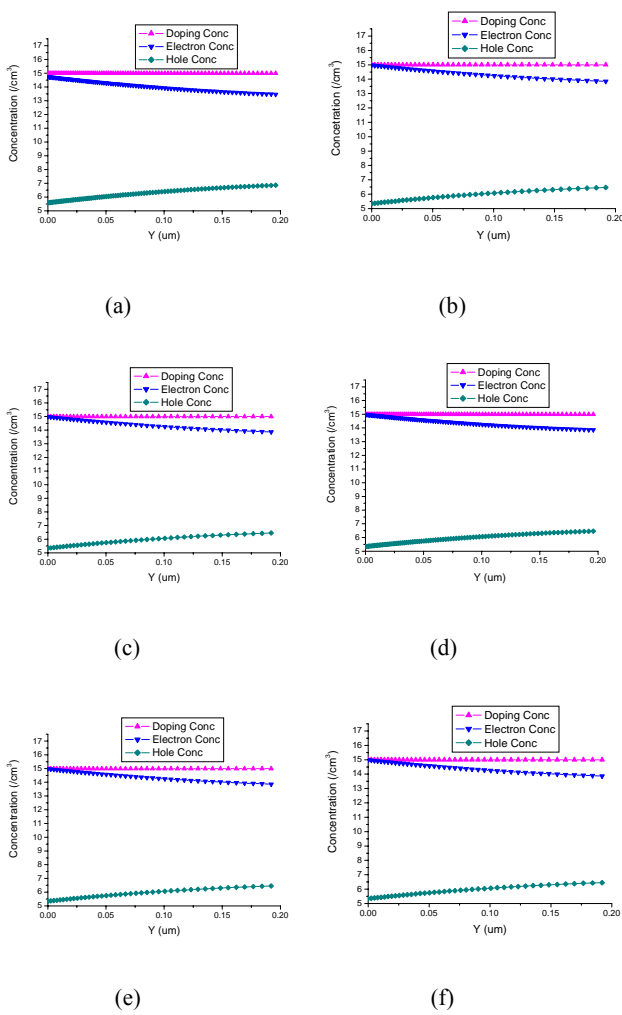
World Academy of Science, Engineering and Technology
International Journal of Physical and Mathematical Sciences
Vol:3, No:10, 2009

(a)　　　　　　　　(b)

(c)　　　　　　　　(d)

(e)　　　　　　　　(f)

Fig. 3 Simulation results for the electron and hole concentration profiles at the middle of the channel for V_{GK}=1V. The d_{Si} is equal to 200nm and the active channel lengths are 2μm for (a), 4μm for (b), 6μm for (c), 8μm for (d), 10μm for (e) , and 12μm for (f).

Figure 4 reports output characteristics of the device with different channel lengths and different gate voltages. Not discernible difference under different gate voltages observed in Fig.4(a) can be easily recognized as a result that depletion region in thin film is formed by V_{AK} but not V_{GK} with a channel length L=2μm. A similar behavior is observed in Fig. 4(b) referring to the device with a channel length L=4μm, with depletion effect becoming less pronounced under V_{GK} as the channel length increases. Note that for channel lengths exceeding 6μm, the depletion effect under V_{GK} is not discernible, and pronounced differences are observed under different gate voltages. On the other hand, obvious differences are obtained from V_{GK}=0V to V_{GK}=0.6V and differences from V_{GK}=0.6V to V_{GK}=1.0 V are not discernible, due to weak inversion in thin film under V_{GK} beyonging 0.6V. (channel lengths exceeding 6μm)
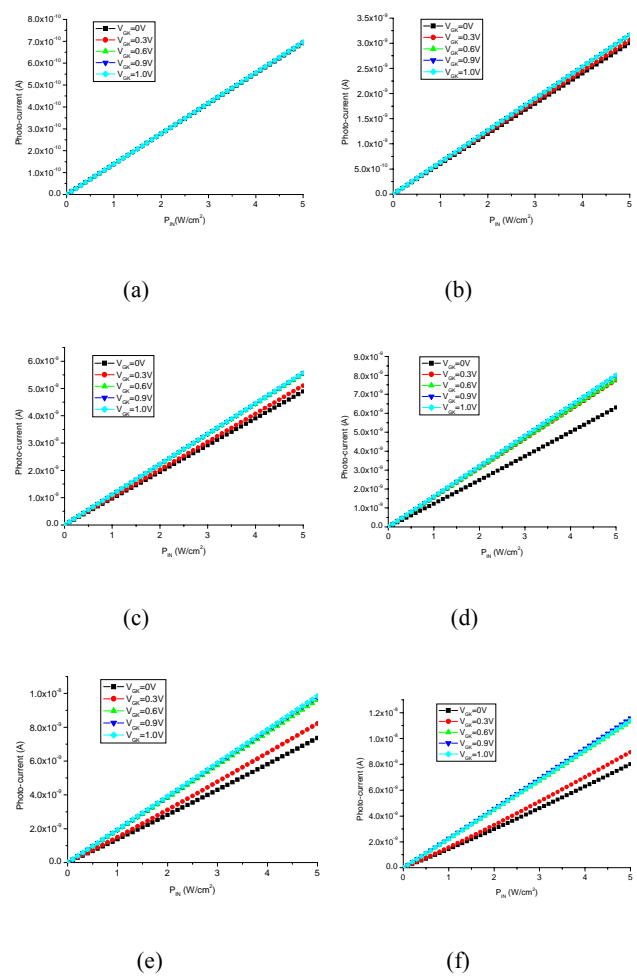

(a)　　　　　　　　(b)

(c)　　　　　　　　(d)

(e)　　　　　　　　(f)

Fig. 4 Photo-current vs illuminating power corresponding to V_{GK}=0V, 0.3V, 0.6, 0.9, 1.0V, respectively, with d_{Si} =200nm and the active channel lengths of (a) 2μm, (b) 4μm, (c) 6μm, (d) 8μm, (e)10μm, and (f)12μm.

Figure.5 shows I-V characteristics of this device in dark for different channel lengths. The dark current is originated from thermionic emission of carriers. It can be seen clearly that dark currents for different channel lengths are horizontal with V_{GK} lower than 0.6V, and increase rapidly exceeding 0.6V. On the other hand, dark current increase pronouncedly for V_{GK} exceeding 10μm. Furthermore, the darkcurrent is increased a little when V_{GK}>0.7V, thus demonstrating that the weak inversion region is formed on the surface.
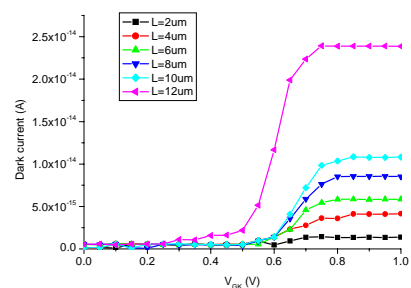

Fig. 5 Dark-current vs V_{GK} arranging from 0.0V to 1.0V with d_{Si}

World Academy of Science, Engineering and Technology
International Journal of Physical and Mathematical Sciences
Vol:3, No:10, 2009

TABLE I
THE DARK-CURRENT, PHOTOCURENT, AND PHOTO-TO-DARK-CURRENT CONTRAST RATIOS UNDER 5W/CM^2 LIGHT INTENSITY AND V_{GK}=0.6V

Channel length(μm)	Photocurent (A)	Dark-current (A)	Photo-to-dark-current contrast ratios
2	6.95e-10	4.56e-16	1.52e6
4	3.16e-09	1.38e-15	2.29e6
6	5.53e-09	1.41e-15	3.92e6
8	8.0e-09	1.41e-15	5.67e6
10	9.61e-09	1.41e-15	6.82e6
12	1.13e-08	1.17e-14	9.66e5

=200nm and the active channel lengths L=2μm, 4μm, 6μm, 8μm, 10μm, respectively.

The dark-current, photocurent, and photo-to-dark-current contrast ratios under 5W/cm^2 light intensity and V_{GK}=0.6V for photo-BJMOSFET are listed in Table I, which indicates that photo-current and dark current both increase along with increasing channel length. The greatest photo-to-dark-current contrast ratio is achieved at L=10μm.

Reports output characteristics of the device with different film thicknesses and different gate voltages for L=10μm are depicted in figure 6. It is indicated that photocurrent increases along with increasing film thickness under the same V_{GK}. However, influences of V_{GK} under different film thicknesses are pronounced and similar with each other.
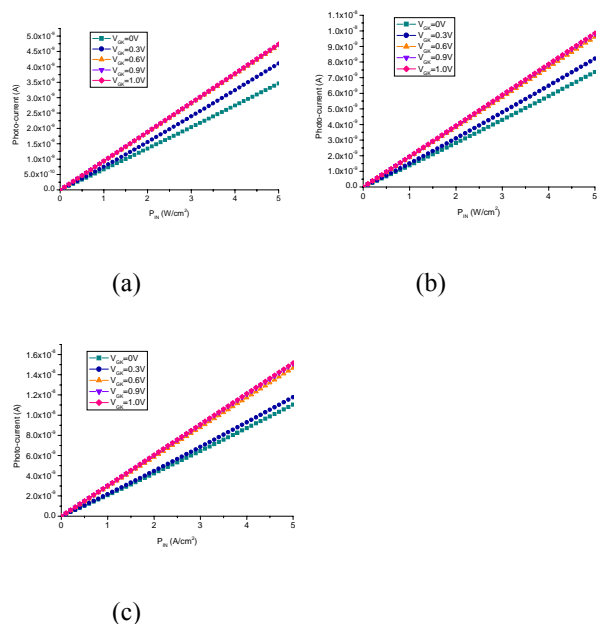

(a)

(b)

(c)

Fig.6 Photo-current vs illuminating power corresponding to VGK=0V, 0.3V, 0.6, 0.9, 1.0V, respectively, with L=10μm and the thin Si film thickness of (a) 100nm, (b) 200nm, and (c)300nm.

Figure.7 shows I-V characteristics of this device in dark for different film thicknesses. It can be seen clearly that dark currents for different film thicknesses are horizontal with V_{GK} lower than 0.6V, and increase rapidly exceeding 0.6V. Furthermore, the darkcurrent is increased a little when V_{GK}>0.7V, thus demonstrating that the weak inversion region is formed on the surface.
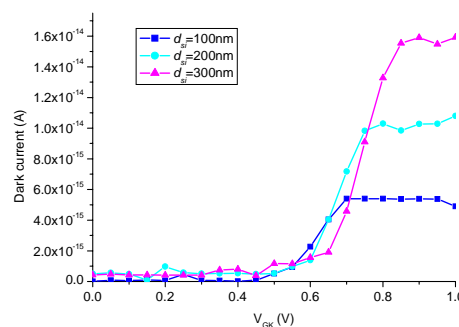

Fig. 7 Dark-current vs V$_{GK}$ arranging from 0.0V to 1.0V with L=10μm and the thin Si film thickness d_{Si} =100nm, 200nm, 300nm, respectively.

IV. CONCLUSION

ITO film which transmittancea is higher than 80% for λ from 500nm to 700nm is adopted as gate in photo-BJMOSFET fabricated on SOI film to reduce light absorption. Thin film is in depletion but not inversion region by gate voltage. I-V characteristics of photo-BJMOSFET obtained in dark (dark current) and under 570nm illumination (photo current) are studied furthermore to achieve high photo-to-dark-current contrast ratio. Numerical simulations are performed by 2D Atlas. Gummel-Newton-based numerical algorithms were implemented and used by the simulation program in order to solve the discretized form of the field equations. Two variables in the calculation were the channel length and the thickness of the film which were set equal to six different values, i.e., L=2, 4, 6, 8, 10, and 12μm and three different values, i.e., d_{si} =100, 200 and 300nm, respectively. The results indicate that obvious performance is observed when channel lengths exceed 6μm and dark currents for different film thicknesses are horizontal with V_{GK} lower than 0.6V, and increase rapidly exceeding 0.6V. Thus, the greatest photo-to-dark-current contrast ratio is achieved with L=10μm and d_{si}=200 nm at V_{GK}=0.6V.

REFERENCES

[1] SM Csutak, JD Schaub, WE Wu, R Shimer, JC Campbell, "CMOS-compatible high-speed planar silicon photodiodes fabricated on SOI substrates," *IEEE J Quantum Electron*, vol.38, pp.193–196, Feb 2002.

World Academy of Science, Engineering and Technology
International Journal of Physical and Mathematical Sciences
Vol:3, No:10, 2009

[2]   Lin Kea, Xin Yue Zhaoa, Ramadas Senthil Kumara and Soo Jin Chua, "Low frequency optical noise from organic light emitting diode," *Solid-State Electronics*, vol.52, pp.7-10, Jan 2008.

[3]   S Nakaharai, T Tezuka, N Hirashita, E Toyoda, Y Moriyama, N Sugiyama, et al "The generation of crystal defects in Ge-on-insulator (GOI) layers in the Ge-condensation process," *Semiconductor science and technology*, vol. 22, pp. 26-28, Jan 2007.

[4]   K. Wang, Y. Vygranenko and A. Nathan, "Optically transparent ZnO-based n–i–p ultraviolet photodetectors," *Thin Solid Films*, vol.515, pp. 6981-6985, June 2007.

[5]   HS Wong, Y Heights, " Technology and device scaling considerations for CMOS imagers,"*IEEE Trans.Electron Devices*, vol.43, pp.2131-2142, Dec 1996

[6]   Nh Zhu, Y Liu, SJ Zhang, JM Wen, "Bonding-wire compensation effect on the packaging parasitics of optoelectronic devices," *Microwave and Optical Technology Letters*, vol.48, pp. 76-79, Jan 2006.

[7]   Y. W. Park and S. Rhee, "Study of a line width estimation model for laser micro material processing using a photodiode," *Optics & Laser Technology*, vol.39, pp. 1461-1471, July 2007.

[8]   S. D. Gunapala, S. V. Bandara, J. K. Liu, E. M. Luong, S. B. Rafol, J. M. Mumolo, D. Z. Ting, et al, "Quantum well infrared photodetector research and development at Jet Propulsion Laboratory" I*nfrared Physics & Technology*, vol.50, pp.211-216, Feb 2007.

[9]   A. J. Blanksby, M. J. Loinaz, "Performance analysis of a color CMOS photogate image sensor," *IEEE Trans ,Electron Devices*, vol.47, pp.55-64, Jan 2000.

[10]   Fábio Alencar Mendonça, Rubens Viana Ramos, "Optical receiver for instrumentation and communication," *Microwave and Optical Technology Letters*, vol. 45, pp. 415-419, May 2005.

[11]   ATLAS Users Manual, SILVACA, Inc.,Santa Clara, CA, 2003

[12]   A. T. Hatzopoulos, N. Arpatzanis, D. H. Tassis, C. A. Dimitriadis , F. Templier, M. Oudwan et al, "Electrical and noise characterization of bottom-gated nanocrystalline silicon thin-film transistors," *J. Appl. Phys*, vol.100, pp.114-117, Dec 2006.

Hai-Qing Xie was born in Hunan, P.R.China, in 1982. He received the degree of Master in Microelectronics and Solid-State Electronics in Hunan University in 2004. He is currently pursuing the Ph.D. degree at the same university, working on optical detectors.

His main research interests concern semiconductor optoelectronic material device and its application